SUPPORTING INFORMATION

Mechanically tunable exchange coupling of Co/CoO bilayers on flexible muscovite substrate

Thai Duy Ha[a,b], Min Yen[c], Yu-Hong Lai[c], Chang-Yang Kuo[b,d], Chien-Te Chen[d], Arata Tanaka[e], Li-Zai Tsai[f], Yi-Feng Zhao[g], Chun-Gang Duan[g], Shang-Fan Lee[f], Chun-Fu Chang[b], Jenh-Yih Juang*[a], Ying-Hao Chu*[a,c,f]

[a] *Department of Electrophysics, National Chiao Tung University, Hsinchu 30010, Taiwan*
[b] *Max-Planck Institute for Chemical Physics of Solids, Nöthnitzer Strabe 40, Dresden 01187, Germany*
[c] *Department of Materials Science and Engineering, National Chiao Tung University, Hsinchu 30010, Taiwan*
[d] *National Synchrotron Radiation Research Center, Hsinchu, 30076, Taiwan*
[e] *Department of Quantum Matter, ADSM, Hiroshima University, Higashi-Hiroshima 739-8530, Japan*
[f] *Insitute of Physics, Academia Sinica, Taipei 11529, Taiwan*
[g] *Department of Electronic Engineering, East China Normal University, Shanghai, China*
*Emails: jyjuang@cc.nctu.edu.tw; and yhchu@g2.nctu.edu.tw

Figure S1. Temperature and pressure dependence of oxide-MBE deposition (a) XPS and (b) XRD spectra of films grown in varied oxygen pressures at 260 °C; (c) XPS and (d) XRD spectra of films grown at varied temperatures in oxygen pressure of 10^{-6} mbar.

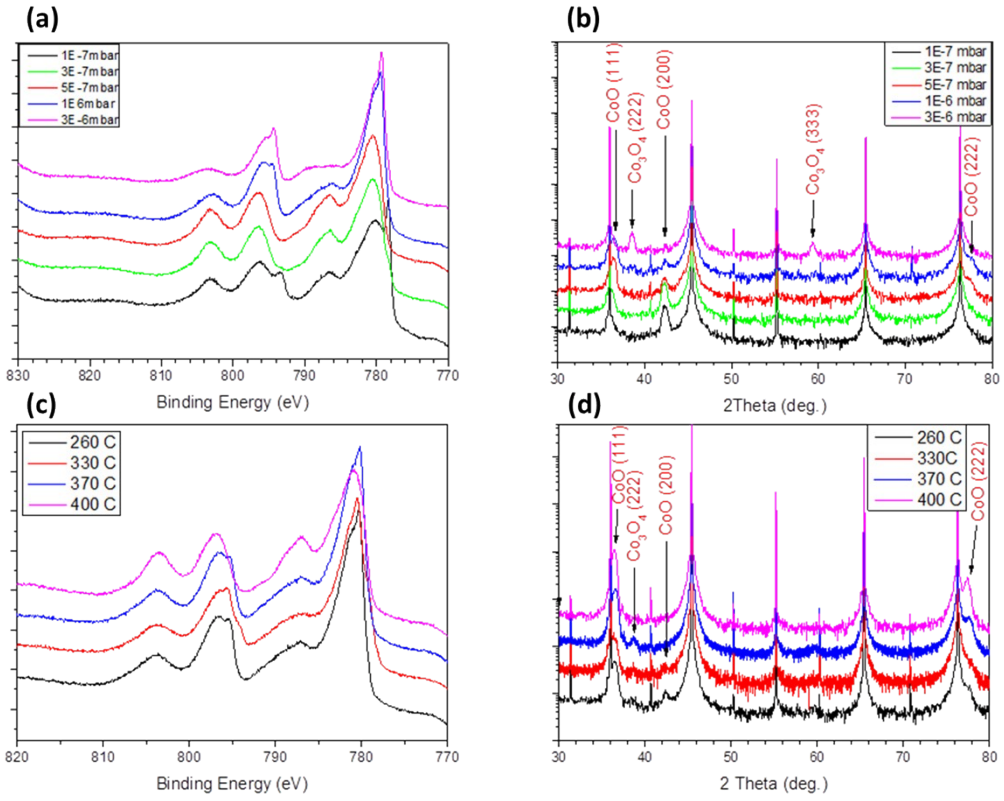

Figure S2. The quality of CoO/mica films by checking the rocking-curve (a) CoO(111)/mica; (b) CoO(100)/mica

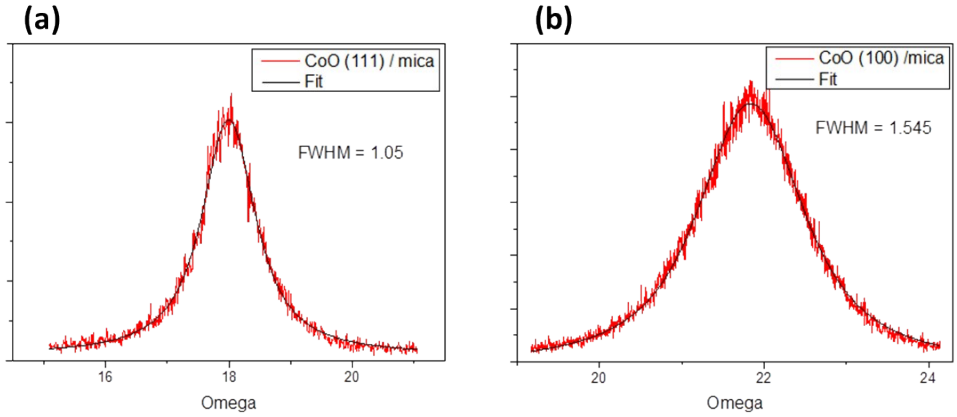

Figure S3. The Raman spectra of CoO films with/without bending.

The Raman spectra of (a) CoO (111); and (b) CoO (100) films on mica substrate were collected during bending-out with various stages. The radius was changed from 12.5 mm to 3.5 mm.

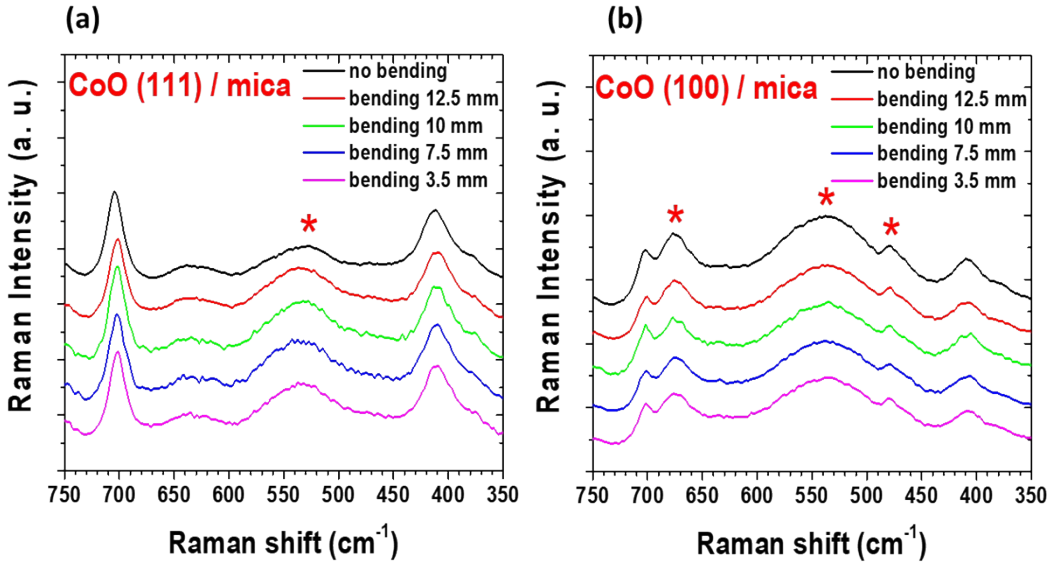

Figure S4. Temperature and thickness dependence of exchange coupling in Co/CoO (111). M-H loops at 50 K, 200 K and 300K of: **(a)** Co_{15nm}/CoO_{20nm}, **(b)** Co_{5nm}/CoO_{30nm}, and **(c)** Co_{5nm}/CoO_{20nm}; **(d)** Extracted H_{EB}.

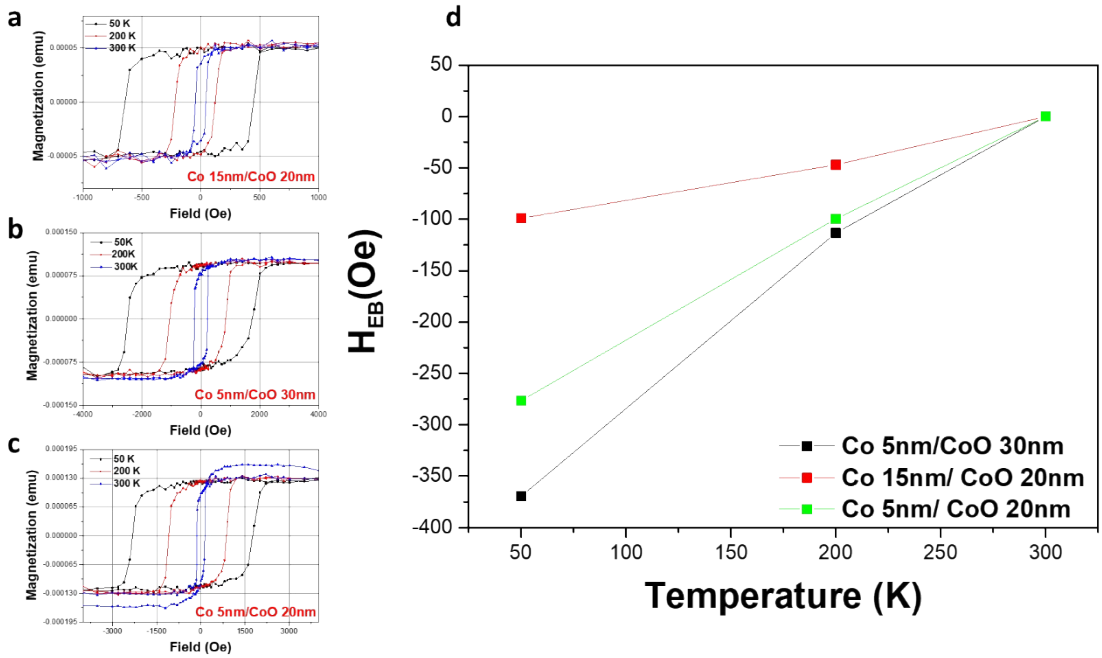

Figure S5. M-H loops of Co/CoO (100) film at different temperatures, different bending radii. (a) Illustration of the bending tests: samples were measured when non-bended, bended-in, bended-out and released; (b)-(f) M-H loops at different temperatures with varied bending states: no bend, bend in with radius of 3 mm, bend out with radius of 3 mm, bend in with radius of 2 mm, bend in with radius of 2 mm, respectively.

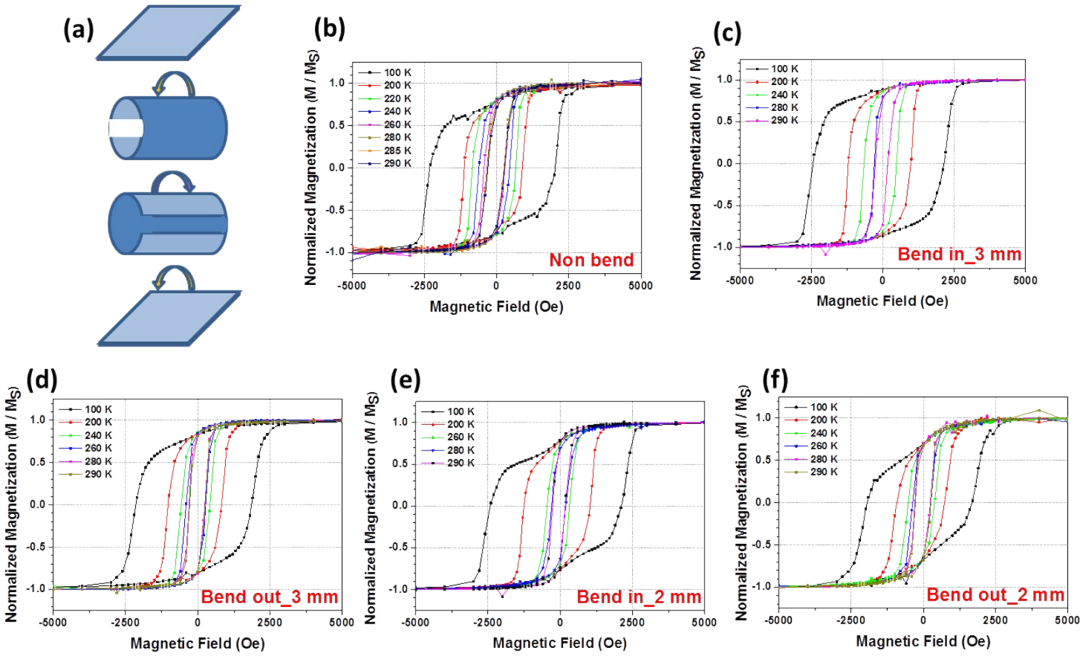

Figure S6. M-H loops of Co/CoO(111) film at different temperatures, different bending radii. (a)-(c) M-H loops at different temperatures with varied bending states: no bend, bend in with radius of 3 mm, bend out with radius of 3 mm, respectively.

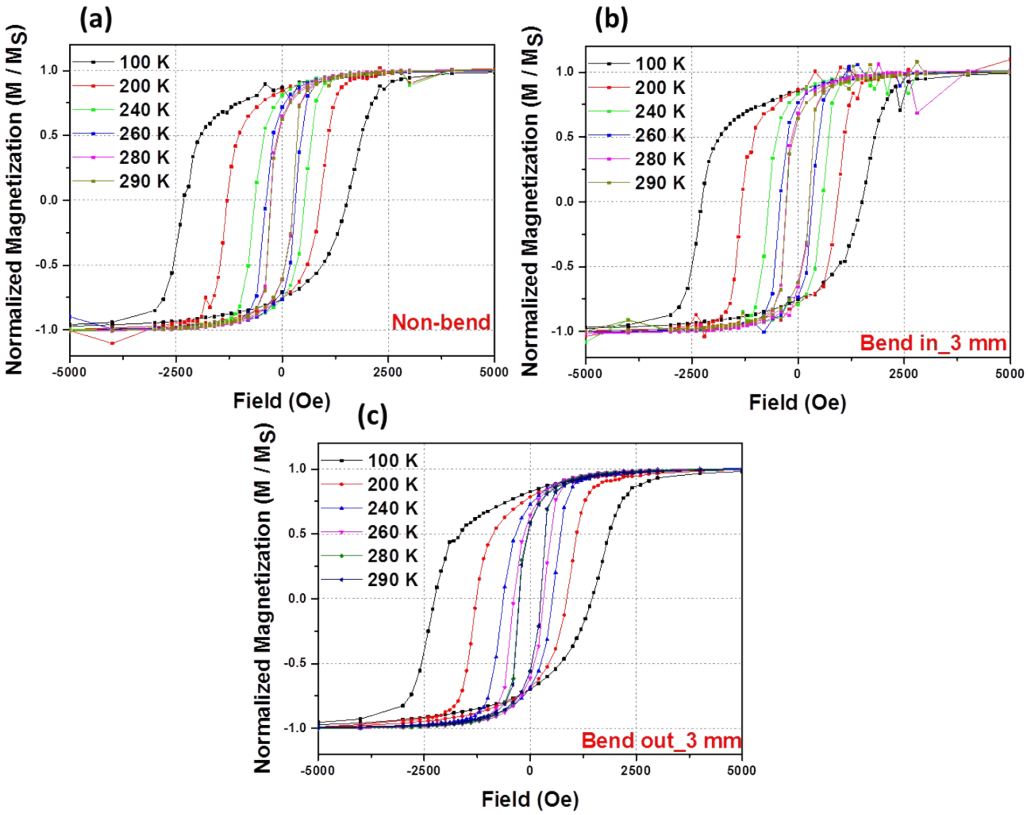

Figure S7. Schematics of AMR measurements (a) Illustration of measurement setup: samples were bended by a cylinder, the applied field was perpendicular to the excitation current; (b) the geometry of measurements: the excitation current was along y-axis, samples were rotated along x-axis, and applied field was along z-axis.

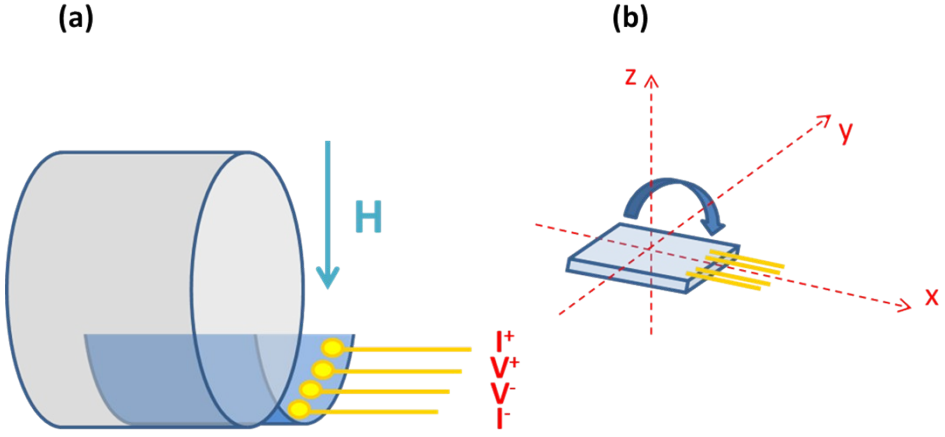

Figure S8. (a) Schematics of conventional epitaxy and vdW epitaxy; (b) RHEED patterns of mica and CoO(111) film; (c) Real-time monitoring RHEED intensity of the growth; (d) Thickness dependence of XAS for CoO(111) films on mica, in comparisons with CoO bulk.

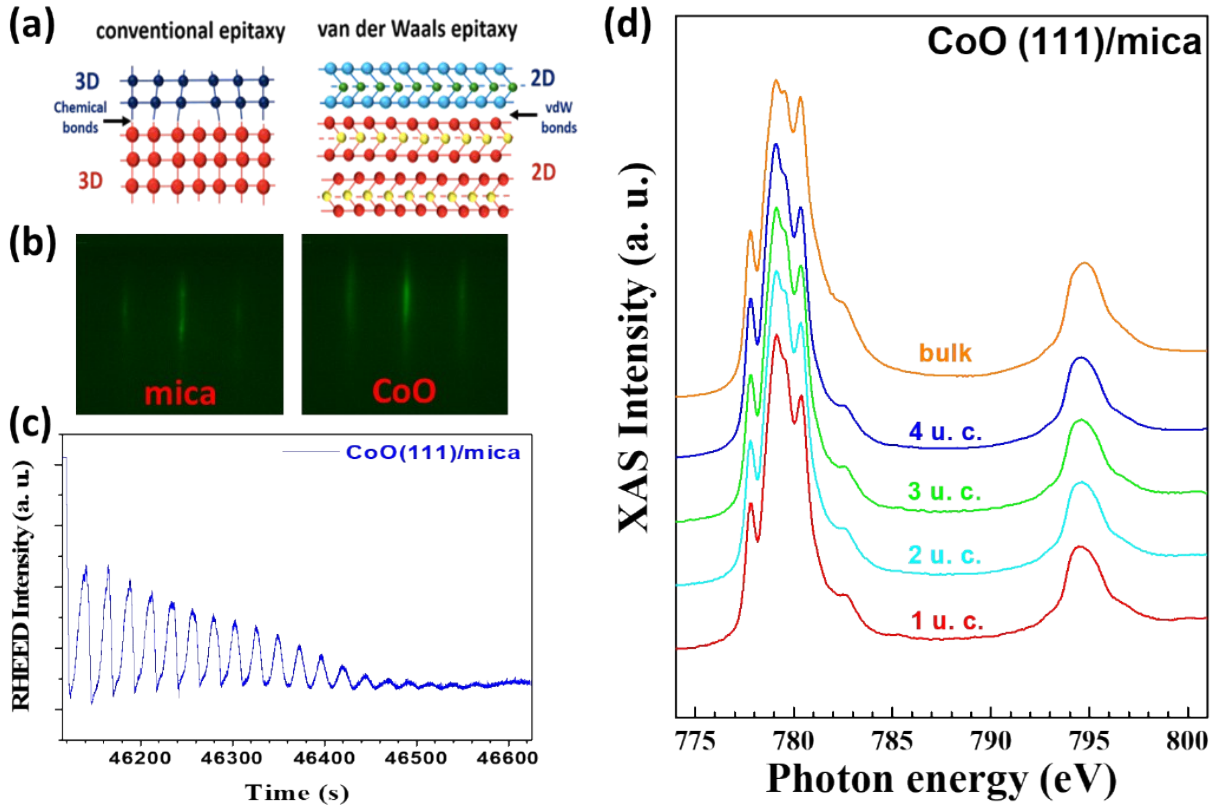

Computational details

First-principles calculations were carried out with the Vienna *ab initio* Simulation Package (VASP)[1] by using the projector-augmented wave (PAW) method[2] and the generalized gradient approximation(GGA).The exchange-correlation potential is adopted in the PBE[3] (Perdew-Burke-Ernzerh) form of GGA+U[4] method with U=7.1eV and J=1eV for cobalt 3d electrons. Both structural relaxation and self-consistent calculations were carried out with the tetrahedral method with Blöchl corrections[5], and the energy cut-off is set to 500eV. We fully optimize each ionic position until the residual forces converged less than 0.001 eV/Å and self-consistent convergence for electronic energy is 10^{-6} eV. A 3×3×3 and 7×7×2 Monkhorst-Pack k-point mesh are adopted for CoO (100) and CoO (111) calculations, respectively.

The calculated lattice constant of 4.261 Å is very close to experimental lattice parameter. We use a 2×2×2 supercell to simulate the type-II AFM structure of CoO (100). And for CoO (111), the bulk structure restructured along [111] direction. Figure S9 shows the atomic structures of CoO (100) and CoO (111). In consideration of applying strain, the lattice parameter of ab-plane is artificially altered. Then we newly relax the c/a of the structures that are used to calculate the MAE.

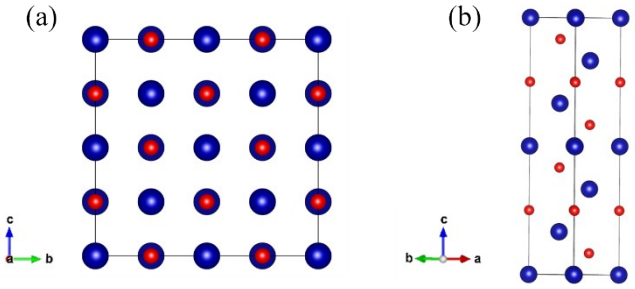

Figure S9. The atomic structure of (a) CoO (100) and (b) CoO (111). Bule and red spheres represent Co and O atoms, respectively.

The main origin of the magnetic anisotropy is the spin-orbit coupling (SOC)[6]. In this work, the calculations about MAE include two steps: first, the charge density is obtained through self-consistent calculations without the spin-orbital coupling. Then, we calculate the total energy for different magnetization axes, for which we use the same charge density and include the spin-orbital coupling.

For CoO without stress, the easy axis is along [001] (or [100], [010]) direction. When the (001) strain is applied, however, the easy axis will be canted away from [001] direction. As shown in Table 1, the magnetic anisotropy energy ($E_{[001]\text{-}[011]}$) changes from negative (strain free) to positive (0.5% strain), suggesting the canting of the easy axis. However, when a 0.5% strain is applied in the (111) plane, the MAE remains negative, meaning that the easy axis is unchanged (Table 1). These calculated results are in nice agreement with the experiments.

Table 1. The calculated magnetic anisotropy energies (MAE, in units of meV) of CoO under (100) and (111) strain. The MAE is calculated as $E_{[001]\text{-}[011]}$.

	(001)	(111)
0%	-7.08	-7.08
0.5%	5.01	-6.66

References

1. Kresse, G.; Furthmuller, J. *Comp Mater Sci* **1996,** 6, (1), 15-50.
2. Blöchl, P. E. *Phys Rev B* **1994,** 50, (24), 17953-17979.
3. Perdew, J. P.; Burke, K.; Ernzerhof, M. *Phys Rev Lett* **1996,** 77, (18), 3865-3868.
4. Anisimov, V. I.; Poteryaev, A. I.; Korotin, M. A.; Anokhin, A. O.; Kotliar, G. *J Phys-Condens Mat* **1997,** 9, (35), 7359-7367.
5. Blöchl, P. E.; Jepsen, O.; Andersen, O. K. *Phys Rev B* **1994,** 49, (23), 16223-16233.
6. van Vleck, J. H. *Physical Review* **1937,** 52, (11), 1178-1198.